GEOLOGICA CARPATHICA, AUGUST 2015, 66, 4, 257–268 doi: 10.1515/geoca-2015-0024

Crystal size and shape distribution systematics of plagioclase and the determination of crystal residence times in the micromonzogabbros of Qisir Dagh, SE of Sabalan volcano (NW Iran)

HAMED POURKHORSANDI[1,2]✉, HASSAN MIRNEJAD[1,3], DAVOUD RAIESI[1] and JAMSHID HASSANZADEH[4]

[1]Department of Geology, Faculty of Sciences, University of Tehran, Tehran 14155–64155, Iran; hmirnejad@ut.ac.ir; davood.raeisi@ut.ac.ir
[2]CEREGE UM34, CNRS, Aix-Marseille University, 13545 Aix-en-Provence, France; ✉pourkhorsandi@cerege.fr
[3]Department of Geology and Environmental Earth Sciences, Miami University, Ohio 45056, USA
[4]Division of Geological and Planetary Sciences, California Institute of Technology, Pasadena, CA 91125, USA; jamshid@caltech.edu

(Manuscript received October 2, 2014; accepted in revised form June 23, 2015)

Abstract: The Qisir Dagh igneous complex occurs as a combination of volcanic and intrusive rocks to the south-east of the Sabalan volcano, north-western Iran. Micromonzogabbroic rocks in the region consist of plagioclase, alkaline feldspar and clinopyroxene as the major mineral phases and orthopyroxene, olivine, apatite and opaque minerals as the accessory minerals. Microgranular and microporphyritic textures are well developed in these rocks. Considering the importance of plagioclase in reconstructing magma cooling processes, the size and shape distribution and chemical composition of this mineral were investigated. Based on microscopic studies, it is shown that the 2-dimensional size average of plagioclase in the micromonzogabbros is 538 micrometers and its 3-dimensional shape varies between tabular to prolate. Crystal size distribution diagrams point to the presence of at least two populations of plagioclase, indicating the occurrence of magma mixing and/or fractional crystallization during magma cooling. The chemical composition of plagioclase shows a wide variation in abundances of Anorthite-Albite-Orthoclase (An = 0.31–64.58, Ab = 29.26–72.13, Or = 0.9–66.97), suggesting a complex process during the crystal growth. This is also supported by the formation of antiperthite lamellae, which formed as the result of alkali feldspar exsolution in plagioclase. The calculated residence time of magma in Qisir Dagh, based on 3D crystal size distribution data, and using growth rate $G = 10^{-10}$ mm/s, varies between 457 and 685 years, which indicates a shallow depth (near surface) magma crystallization and subvolcanic nature of the studied samples.

Key words: Iran, Sabalan, Qisir Dagh, subvolcanic rocks, magma mixing, crystal size distribution.

Introduction

The textures and chemical compositions of magmatic rocks provide important information about magmatic processes. The type of texture in igneous rocks depends on the rate of magma cooling and crystal nucleation, growth rates and residence time (Winkler 1949; Vernon 2004). Most of the routine textural investigation on igneous rocks deals with the description of crystal shapes, the relationship of components with each other and the relative size of crystals, all of which are often reported as qualitative data (Seasman 2000; Higgins 2000; Innocenti et al. 2013). To investigate three-dimensional state of grains, Randolph & Larson (1971) proposed the Crystal Size Distribution (CSD) theory for synthetic solids, which was later developed by Marsh (1988) and applied to magmatic systems and the resultant igneous rocks. By using CSD theory, valuable information on the ratio and density of nucleation, crystallization degree, growth rate and magma cooling process can be achieved. Some noteworthy studies on the application of CSD to terrestrial rocks such as crystal shapes and defining new models to simulate solidification of magma were done in the 1990s (e.g. Marsh 1988; Armienti et al. 1991; Cashman 1993; Higgins 1994; Sahagian & Proussevitch 1998). In most of CSD studies on igneous rocks, measurements have been focused on plagioclase, because it is the most frequent mineral in igneous rocks, is stable in a wide spectrum of magmatic conditions, and can record physico-chemical fluctuations within a magma chamber (Gagnevin et al. 2007; Ruprecht & Wörner 2014).

Cenozoic magmatic activities in NW Iran are closely linked to the collision between the Afro-Arabian and Eurasian plates (Berberian & King 1981). The Eastern Azerbaijan region of Iran is part of a vast igneous province that is situated between two inland seas, the Caspian Sea and Black Sea (Innocenti et al. 1982; Dilek et al. 2010). The Qisir Dagh igneous suit, located between Sarab and Nir cities in NW Iran, is mainly composed of basaltic and andesitic volcanic rocks. Didon & Gemain (1976) reported a "dioritic" igneous mass in Qisir Dagh. However, there are no adequate data on the occurrence, formation and the relationship of these rocks with the other igneous rocks in the region.

The aim of this study is to understand the crystallization kinetics of magma by means of physical and chemical observations and to use them to infer the crystallization processes of the studied rocks. The dynamics and history of magma cooling in Qisir Dagh, including the solidification mechanism of the magma chamber and the emplacement level (i.e. volcanic versus

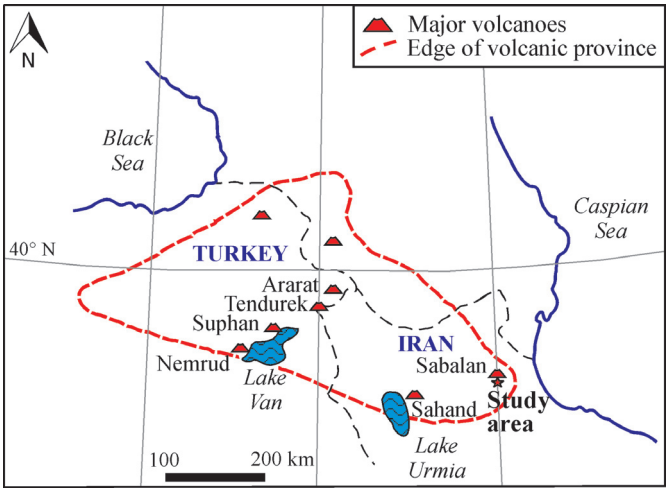

subvolcanic) in the associated magmatic system are investigated by employing quantitative and qualitative petrography, mineral chemistry and CSD of plagioclase crystals from micromonzogabbros in the Qisir Dagh igneous suit.

General geology

The Iranian plateau is tectonically an active region within the Alpine-Himalayan orogenic belt. Closure of the Neotethys ocean as a result of the northward motion

Fig. 1. Map showing the geographical location of the study area relative to the nearby large stratovolcanoes (modified after Lambert et al. 1974 and Dostal & Zerbi 1978).

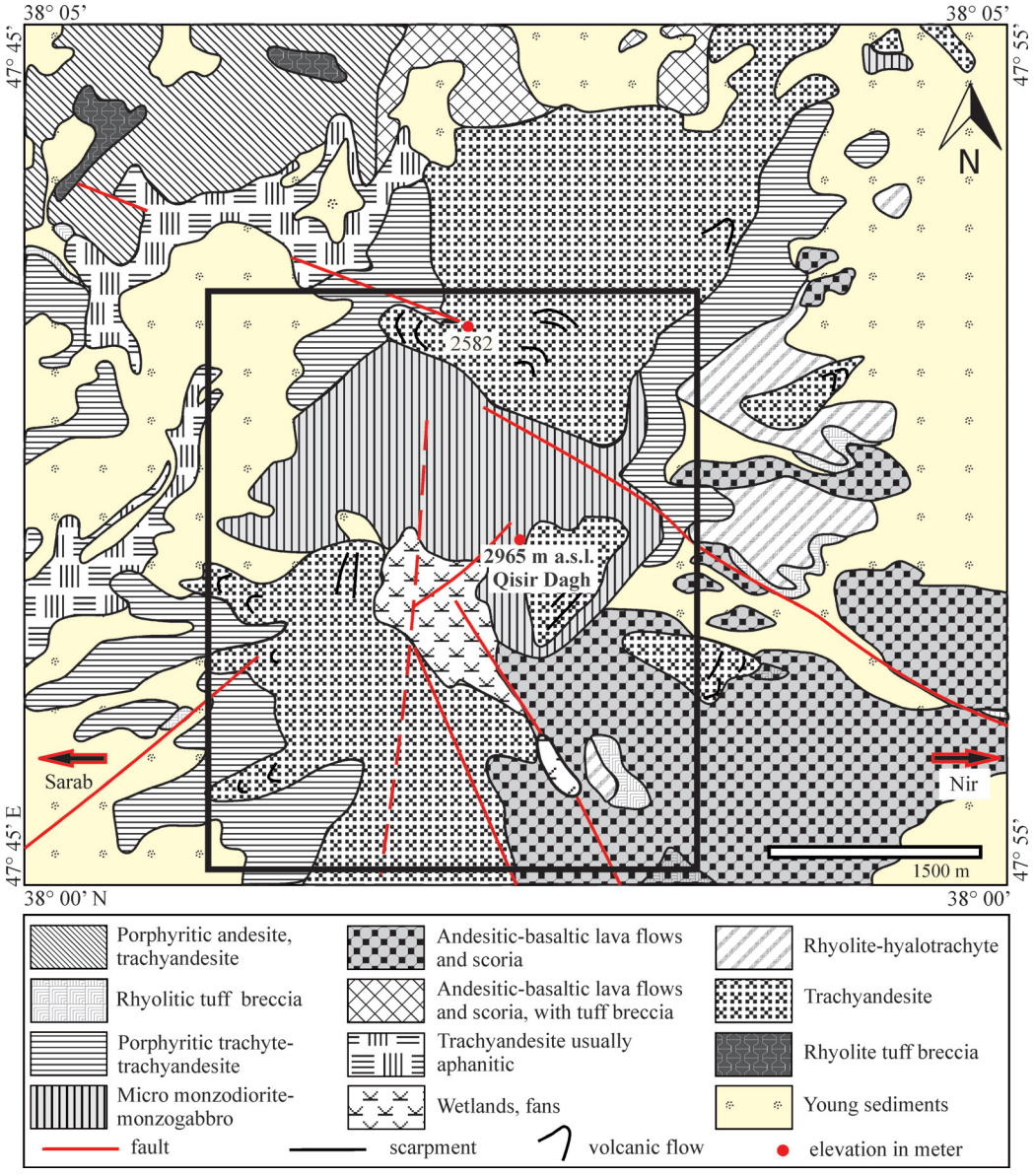

Fig. 2. Geological map of Qisir Dagh and the surrounding region. The highest point marks Qisir Dagh's peak. Quadrangle shows the volcano (Simplified after Amini 1987).

of the Afro-Arabian plate and the associated subduction beneath the southern margin of Eurasia in the Late Mesozoic and Early Cenozoic had a major role in the evolution of continental crust in Iran (Stöcklin 1968; Takin 1972; McQuarrie et al. 2003; Allen et al. 2011). These tectonic events led to the development of Urumieh-Dokhtar Magmatic Arc (UDMA), Sanandaj-Sirjan Metamorphic Zone (SSMZ) and Folded Zagros Zone (FZZ) in Iran (Ruttner & Stöcklin 1967; Pazirandeh 1973).

Convergent motion between the Afro-Arabian and Eurasian plates triggered intense magmatic activity in the Cenozoic that is particularly distinguished in NW Iran, Anatolian plateau of Turkey, Armenia, Georgia and Azerbaijan. A large igneous province that occupies an area of about 200,000 km^2 and hosts large stratovolcanoes in NW Iran and Eastern Turkey (e.g. Sabalan, Sahand and Ararat), formed as a result of this activity (Fig. 1) (Alberti et al. 1980; Yilmaz et al. 1990; Trifonov et al. 2012; Kheirkhah & Mirnejad 2014). Some researchers suggest that there is a petrogenetic relationship between the Cenozoic magmatism of this igneous province and those of Alborz and UDMA in Iran (Alberti et al. 1976; Innocenti et al. 1982; Jahangiri 2007; Azizi & Moinevaziri 2009; Ahmadzadeh et al. 2010; Allen et al. 2011; Dabiri et al. 2011; Jamali et al. 2012).

Sabalan (4811 m a.s.l.) [Sabalân/Sāvālān] a Plio-Quaternary stratovolcano located in the eastern Azerbaijan region of Iran, is composed of high-K, calc-alkaline andesitic rocks that currently shows hydrothermal activities (Alberti et al. 1975; Didon & Gemain 1976; Dostal & Zerbi 1978; Ghalamghash et al. 2013). The southern lowlands of Sabalan consist of basaltic and andesitic rocks of Cenozoic age, which have reached the surface through temporary volcanic fissures. Contrary to these, Qisir Dagh, a central volcanic structure, is a product of much more durable magmatic activity. The geological map of the region is shown in Fig. 2 (Amini 1987). The Miocene volcanic rocks of Qisir Dagh are overlain by volcanoclastic sediments of the pre-Sabalan stage (Didon & Gemain 1976; Alberti et al. 1976; Amini 1987). Didon & Gemain (1976) suggest that Qisir Dagh is an eroded stratovolcano and the depression which divides it into eastern and western parts is the eroded remnant of a caldera (Fig. 3a,b). In the northeast of the depression, which is the focus of this study, igneous rocks occur as dyke swarms and dome-like structures (Fig. 3c). Fine grained texture and lack of volcanic structures in these rocks suggest a probable subvolcanic origin. Based on changes in colour, structure and weathering degree, four different varieties of micromonzodiorite-monzogabbro are distinguished in the field (Fig. 4a).

Pourkhorsandi (2014) reports a narrow range of SiO_2 content (53.01–56.52 %, average 54.66 %) for these rocks. Considering the classification scheme of Le Bas et al. (1986), the studied rocks from Qisir Dagh belong to the monzodiorite-monzogabbro class of igneous rocks (Fig. 5a). These rocks are silica saturated/oversaturated and show high-K and shoshonitic affinities (Fig. 5b). The Ce/Pb ratio of the studied rock varies between 1.6 and 3.1 (Pourkhorsandi 2014). Compared to the ratio of ~25 for magmas originating from the mantle (Rollinson 1993), this is very low and is similar to the ratio of the upper crustal rocks for which the average is 3.5 (Rollinson 1993).

For evaluating the CSD in the Qisir Dagh igneous rocks, we selected micromonzogabbro samples (Fig. 4b), because the rocks of this group are more widespread and least altered compared to other igneous rocks in the region.

Methodology

Fifty rock samples were collected from igneous units in Qisir Dagh and 30 specimens were selected for petrography and rock classification. Among these, five thin sections from micromonzogabbros were prepared for quantitative optical microscopy. Selected samples had a proper distance from each other

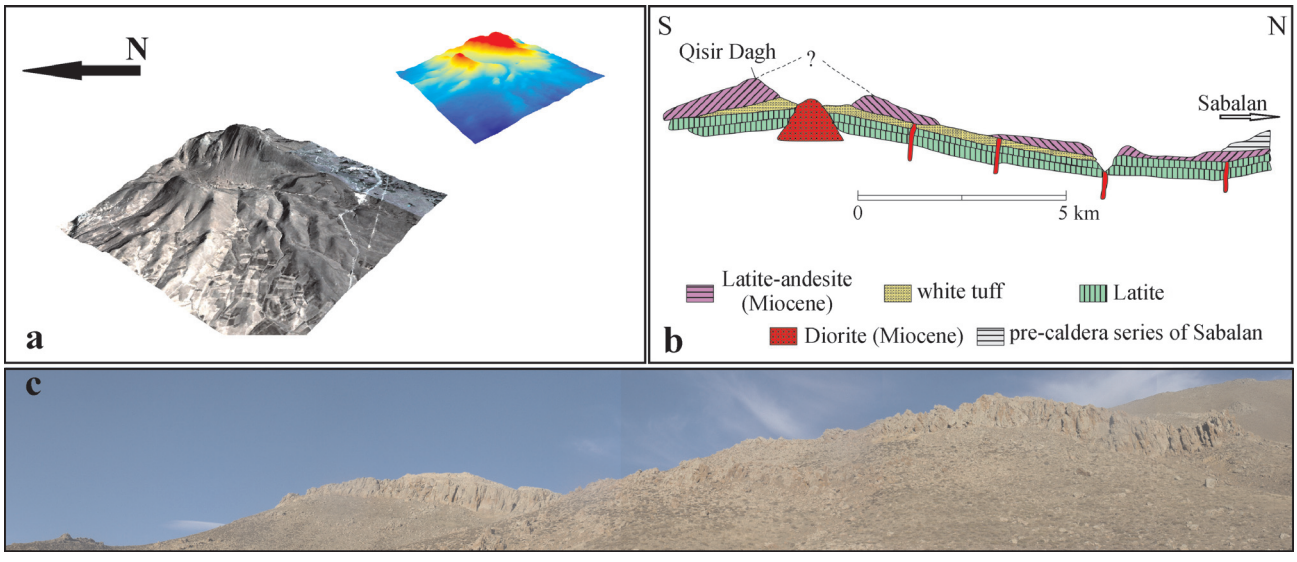

Fig. 3. a — 3D and topographic view of Qisir Dagh (Data source: Google Earth), **b** — geological profile of Qisir Dagh and the position of the studied rocks (diorite in this map) (after Didon & Gemain 1976), **c** — panoramic view of the studied rocks of Qisir Dagh, showing micromonzogabbros as the cliffs.

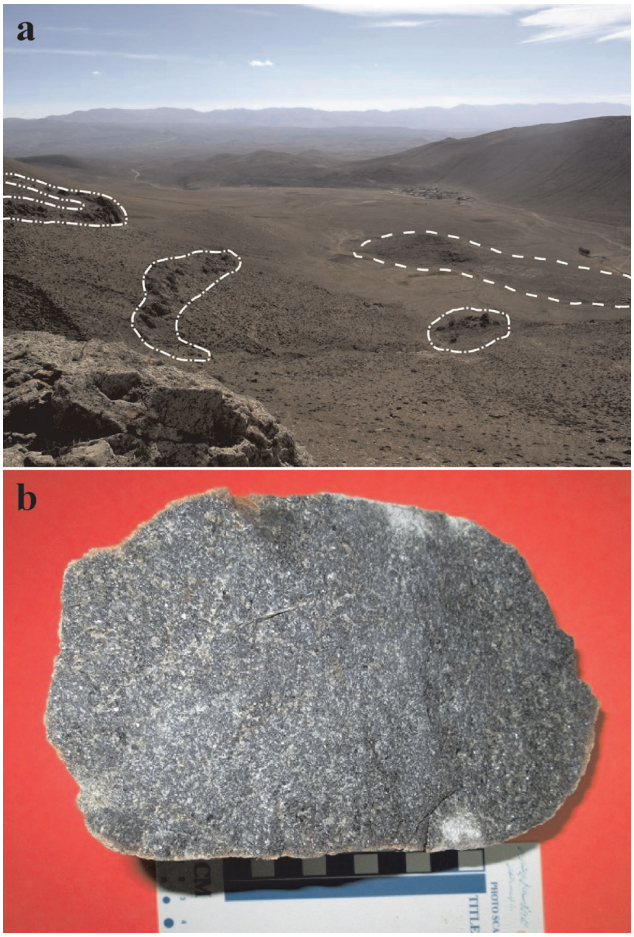

Fig. 4. **a** — Different varieties of micromonzodiorite and micromonzogabbro occur in Qisir Dagh, shown as dashed and dash-dotted line, respectively, **b** — The hand specimen image of micromonzogabbros that was used for CSD study.

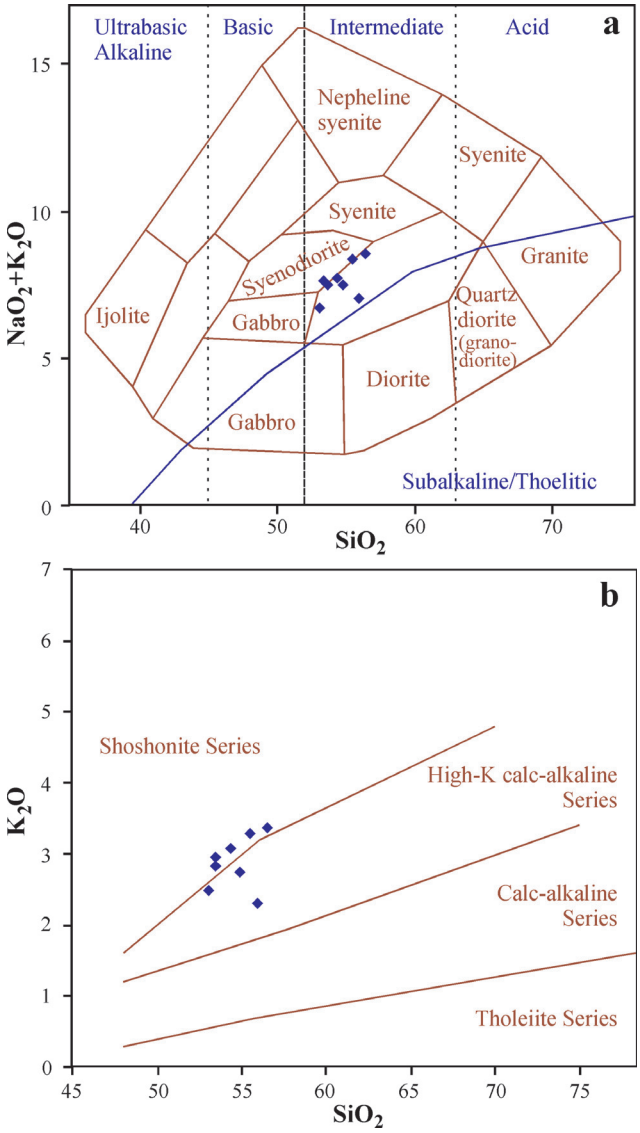

Fig. 5. The position of igneous rocks from Qisir Dagh. **a** — Na_2O+K_2O versus SiO_2 diagram (Cox et al. 1979), **b** — K_2O vs. SiO_2 diagram (Peccerillo & Taylor 1976).

and were the least altered. For two-dimensional size measurements, more than 95 % of the area of a thin section, in X25 magnification (crossed polars) and with and without the presence of a gypsum plate, was photographed. The gypsum plate increases colour contrast between crystals, sharpens mineral outlines and facilitates size measurements. Lamellar twinning and crystal shape of the plagioclase crystals are some of the criteria which were used to differentiate plagioclase from alkali feldspar, while comparing the section under "normal" cross polarized light with the one with gypsum plate inserted. The subvolcanic nature of the studied rocks makes the process of crystal outline distinguishing and measuring difficult. To prevent any false results, crystals with unclear outline were omitted which decreases the number of the crystals to measure. However, the overall number of the measured crystals is more than those reported from elsewhere (e.g. Diaz Azpiroz & Fernandez 2003). To estimate the frequency of different size groups, the length and width of 2266 plagioclase grains were manually and visually measured in the longest perpendicular directions using JMicroVision software platform. Extraction of 3D shape and size distribution data from raw 2D data was done using the CSDSlice5 spreadsheet (Morgan & Jerram 2006) and CSD Corrections 1.4.0 software (Higgins 2000, 2002).

Chemical compositions of feldspars (both plagioclase and alkali feldspar) were determined with JEOL JXA-8200 electron microprobe at the California Institute of Technology, using focused electron beam (~1 micrometer in diameter), an accelerating voltage of 15 kV and a beam current of 25 nA. The data were reduced using the CITZAF algorithm (Armstrong 1988).

Petrography

The studied samples are classified as micromonzogabbros, based on modal mineralogy and texture. The micromonzogabbros in Qisir Dagh consist of plagioclase (65–75 %),

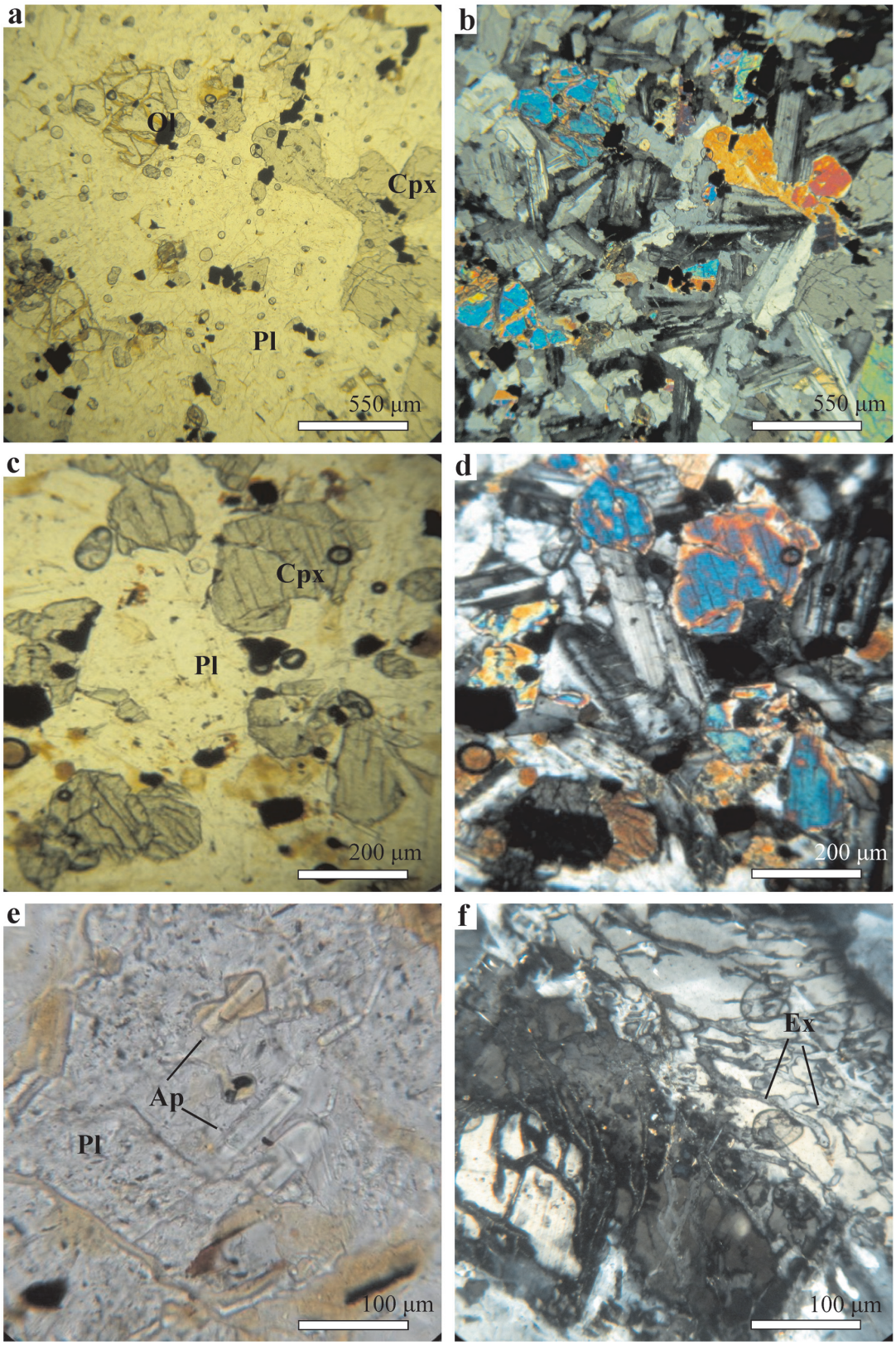

Fig. 6. Microphotographs of thin sections for micromonzogabbros from Qisir Dagh. **a, b** — Parallel and crossed polars images (respectively) of micromonzogabbros. Plagioclase (Pl), alkali feldspar, olivine (Ol) and pyroxene (Opx and Cpx) have formed microgranular texture (scale bar: 550 µm); **c, d** — Clinopyroxene is the most frequent mafic mineral in the studied rocks. PPL and XPL images (respectively) (scale bar: 200 µm); **e** — Elongate apatite (Ap) crystals inside a plagioclase. Note the lineation of the apatite (scale bar: 100 µm); **f** — Exsolution lamellas of feldspar (Ex) inside a more calcic plagioclase crystal (scale bar: 100 µm).

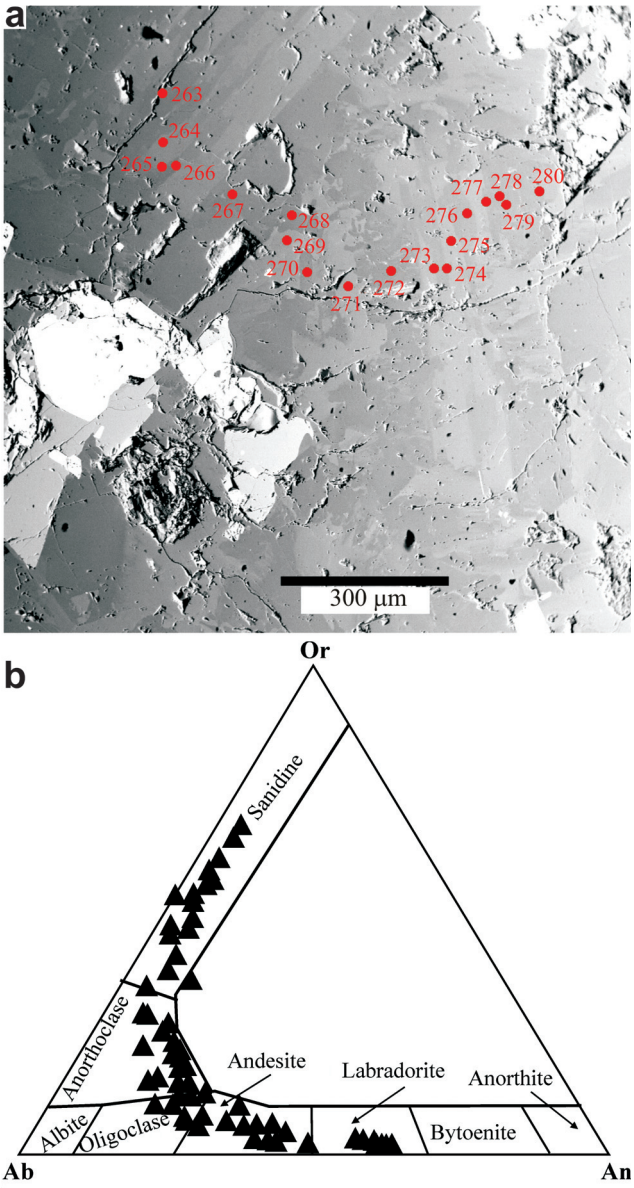

Fig. 7. a — BSI image showing the analysed points in feldspars, showing the changes in BSE image color with changing the composition of feldspar, **b** — Ternary orthoclase-albite-anorthite (Or-Ab-An) diagram showing the position of analysed feldspars from Qisir Dagh micromonzogabbros.

alkali feldspar (10–15 %), olivine (5–10 %), opaque minerals (3 %), clinopyroxene (5 %), orthopyroxene (1 %) and apatite. Microgranular, intergranular and in some cases microporphyritic textures also developed in these samples (Fig. 6a,b).

Plagioclase is euhedral to subhedral and occurs as phenocryst (average 0.2–0.8 mm) and microphenocrysts (<0.1 mm). In some plagioclase grains, exsolution textures occur as irregular dendritic veins of sodic and potassic plagioclase inside calcic varieties of the mineral (Fig. 6f). Subhedral alkali feldspar occurs as phenocryst (0.1–0.7 mm) and is mainly altered to sericite. Subhedral and anhedral crystals of clinopyroxene occur as phenocrysts (~0.5 mm) and as inclusions in plagioclase. Possible instability of clinopyroxene in the presence of magma has led to the development of corrosion textures. Alteration of clinopyroxene to serpentine and opaque minerals is evident from the co-presence of these minerals. Fig. 6a–d shows the opaque and clinopyroxene crystals, mostly in the vicinity of each other. Orthopyroxene is euhedral to subhedral and exhibits smaller sizes relative to clinopyroxene. Olivine (~0.2–0.7 mm) occurs as euhedral to anhedral gains and is commonly altered to iddingsite and serpentine. Most of the apatite crystals in the studied rocks show poikilitic textures, as most are lineated in pyroxene and plagioclase (Fig. 6e).

Mineral chemistry

The microprobe analyses of plagioclase and the calculated cation numbers are presented in Table 1. Fig. 7a shows the backscattered electron (BSE) image of a feldspar and Fig. 7b depicts the range of chemical variations of this mineral in an Or-Ab-An ternary diagram. The brighter patches reflect areas characterized by higher Ca/Na or K/Na ratios. Feldspar ranges in compositions An0.31 to 64.58. In the studied samples, plagioclase normally lacks chemical zoning and shows complex irregular patchy textures. The K content of plagioclase in the studied samples is higher than that of ordinary plagioclase in igneous rocks reported by Deer et al. (1992). High amounts of K can be considered indicative of a complex process that led to the development of exsolution lamellas (e.g. perthite, antipertithe and cryptoperthite) in plagioclase.

Table 1: Microprobe analyses of feldspar in Qisir Dagh samples.

Point#	216	217	218	219	220	221
SiO_2 wt. %	65.80	63.31	52.64	62.47	63.40	65.54
TiO_2	0.10	0.16	0.14	0.12	0.12	0.13
Al_2O_3	19.27	21.55	29.16	22.23	22.44	19.18
FeO	0.34	0.41	0.44	0.44	0.39	0.24
MgO	0.00	0.00	0.02	0.00	0.00	0.00
CaO	0.70	3.36	12.18	4.16	3.93	0.78
Na_2O	4.69	7.27	4.43	7.58	7.20	3.27
K_2O	9.58	3.43	0.38	2.46	3.06	11.41
Cr_2O_3	0.01	0.02	0.00	0.03	0.00	0.00
MnO	0.00	0.01	0.01	0.00	0.00	0.02
Oxide totals	100.50	99.53	99.40	99.48	100.55	100.57
Ab mol %	41.24	63.85	38.82	65.91	63.24	29.16
An	3.38	16.32	58.97	20.02	19.08	3.86
Or	55.38	19.83	2.21	14.06	17.68	66.97

Theory of CSD

CSD deals with the size distribution of crystal populations as a function of the number of crystals in a measured volume and the amount of crystals within a series of defined size intervals (Marsh 1988). Stereology techniques that produce CSD data consist of a body of methods for the exploration of three-dimensional space, when only two-dimensional sections through solid bodies or projections on a surface are available (Underwood 1973).

Mathematically, the crystal population density (n) is defined as $n(L) = dN(L)/dL$, where N(L) is the cumulative number of crystals per unit volume with long axes equal to or lower than L and n is the number of crystals per unit volume in a given size class. Crystal population density is best represented by a plot of ln(n) versus crystal length (L). The histograms of volume fraction (number of crystals for each size) vs. size is another method for representing the CSD data (Higgins 2000; Jerram et al. 2009).

Cashman & Marsh (1988) showed that the shape of the CSD curves could be related to various magmatic processes such as crystal fractionation and accumulation, magma mixing and coarsening. In this study, the program CSDcorrections 1.4.0. was used to produce CSD curves, which convert 2-dimensional intersectional data (length and width) to true 3-dimensional crystal size distributions by incorporating corrections for the intersection probability and cut-section effects. Utilization of this program also requires an estimation of the sample fabric, grain roundness and 3D crystal shape. Based on petrography of five thin sections, a roundness factor of 0.2 is chosen for Qisir Dagh samples. The 3D shapes of the plagioclase crystals from Qisir Dagh were estimated using the CSDSlice 5 spreadsheet (Morgan & Jerram 2006), which compares the distribution of 2D size measurements to a database of shape curves for random sections through 703 different crystal shapes and determines a best fit 3D crystal habit based on regression calculations and fitting to the database. Crystal shapes are defined in terms of "aspect ratio" that is the ratio of short: intermediate: long (S: I: L) dimensions.

As proposed by Marsh (1988), average crystal residence time is calculated by employing the equation:

$$Tr = (-1/G \times m)/31536000$$

where Tr is the residence time (year), G is the growth rate of crystals (mm/s), m is the slope of the CSD curve of the long-linear data and 3156000 is a coefficient to convert seconds to years. Choosing the appropriate growth rate is important for calculating the residence time. Cashman (1993) has considered a growth rate of 10^{-9} mm/s and 10^{-10} mm/s for 3 and 300 years of cooling time, respectively. This author also considers a residence time of less than 1000 years for low-depth magmatic bodies, which are similar in composition to the Qisir Dagh rocks. Based on the strong dependence of calculated residence time to growth rate, we chose the value of 10^{-10} mm/s used by Garrido et al. (2001) and Cheng & Zeng (2013) to calculate sub-volcanic gabbroic magmatic bodies that are not too different from our studied rocks.

CSD results

Distribution of 2D length and width size (intersection dimensions) data of the 2266 measured grains is presented in Table 2 and shown as a frequency versus size histogram in Fig. 8. The two-dimensional size average of plagioclase in

Table 2: Two-dimensional parameters of plagioclase crystals.

Sample	Number of measured crystals	Average length size (μm)
QSD-10b	929	420
QSD-12	418	608
QSD-14	423	569
QSD-17	162	644
QSD-23	334	684

Table 3: Calculated crystal shape parameters. S, I and L represent short axis, intermediate axis and long axis, respectively. S/I (short axis/intermediate axis) and I/L (intermediate axis/long axis).

Sample	Aspect ratio	S/I	I/L	Crystal shape
QSD-10b	1:1.4:2.4	0.71	0.58	Prolate
QSD-12	1:1.5:1.9	0.67	0.79	Tabular
QSD-14	1:1.4:2.4	0.71	0.52	Prolate
QSD-17	1:1.7:2.2	0.59	0.77	Tabular
QSD-23	1:1.7:2.5	0.59	0.68	Tabular

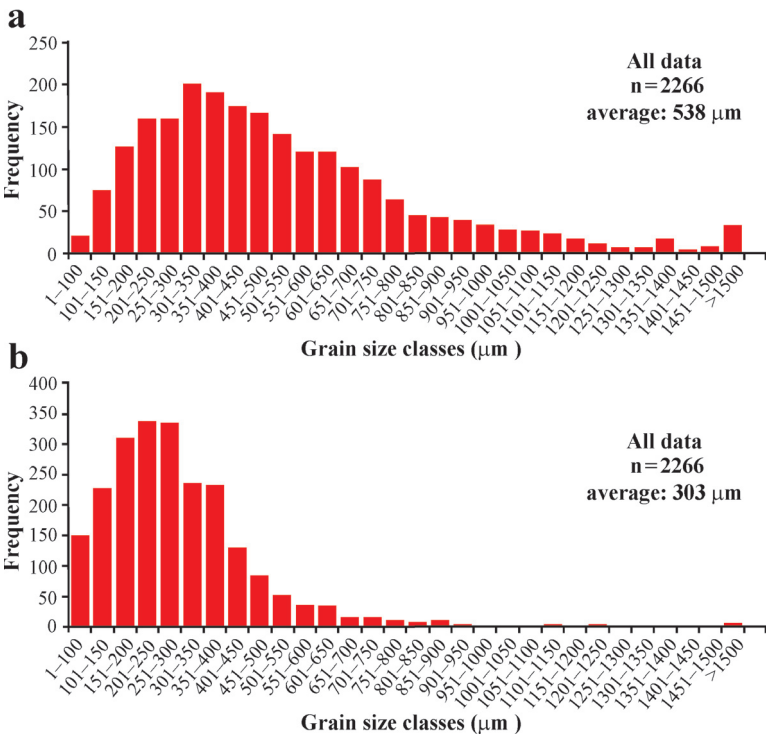

Fig. 8. Frequency versus length (**a**) and width (**b**) histograms of the measured plagioclase grains. Variation in length sizes is more than widths.

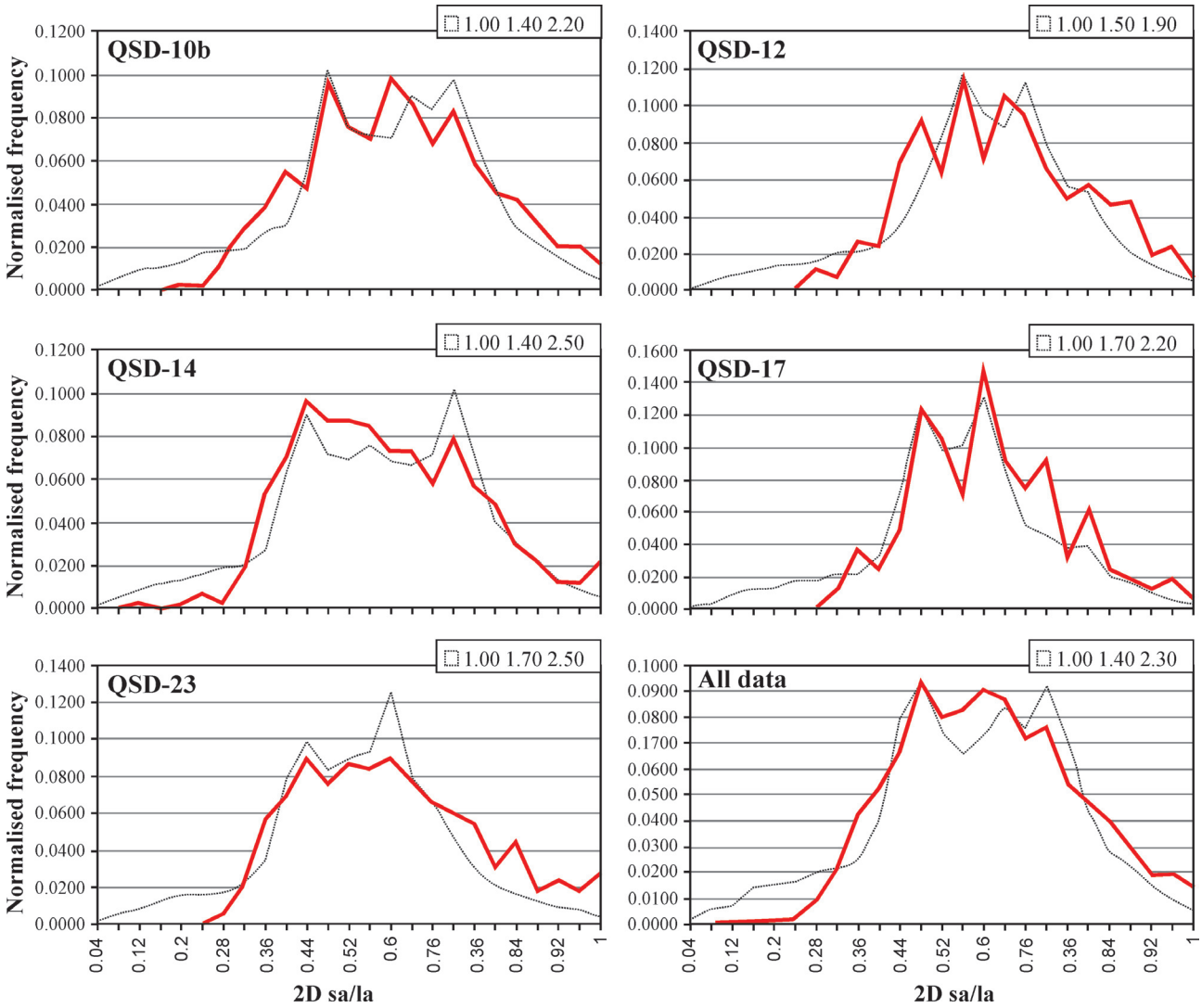

Fig. 9. Frequency versus 2D sa/la (short axis/long axis) histograms of the measured samples from Qisir Dagh (red lines) together with best-fit shape output by CSDSlice (dashed lines) and the proposed aspect ratios. The numbers on the right corner represent the aspect ratios as represented by short axis: intermediate axis: long axis of the crystal.

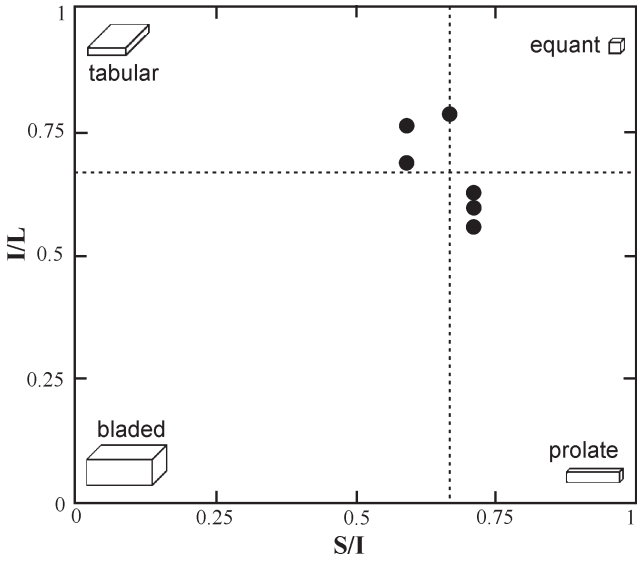

the micromonzogabbros of Qisir Dagh is 538 micrometers. Plagioclase crystals with lengths of less than one millimeter are much more abundant than those having larger sizes. As can be seen in Fig. 8, plagioclase crystals show unequal shapes and their lengths exhibit more variation in sizes than widths. However, we considered the measured plagioclase lengths to be real and not the results of clustering of crystals although this cannot be excluded in the largest size bins (>1500 μm, Fig. 8a), the other reason for this bin could be the presence of xenocrystals. As a result of the fact that larger crystals show higher degrees of K-metasomatism, this reason

Fig. 10. The position of average aspect ratio of plagioclase in igneous rocks on I/L versus S/I diagram (Zingg 1935). Plagioclase from Qisir Dagh (filled cricles) plot in prolate and tabular 3D shapes (excluding one sample that resides between tabular and equant). S, I and L represent small, intermediate and long axis, respectively.

sounds likely. Calculated crystal shape data are presented in Table 3. I/L and S/I factors were calculated from the aspect ratio data. Fig. 9 shows the population shape curves of normalized frequency vs. short axis/long axis ratio together with the best-fit shape output by CSDSlice 5 for the studied samples from Qisir Dagh rocks. Dotted lines are the data of some standard crystals from the data source of CSDSlice 5 and the red lines are our data. Dotted lines show the most similar crystal shapes to our data and have been considered to be similar to our sample crystal factors.

The I/L versus S/I diagram of Zingg (1935) is used here to present the data and to evaluate the 3D shapes. As can be seen in Fig. 10, the majority of the plagioclase crystals are either prolate or tabular in 3D shape, and one sample (QSD-17) is intermediate between tabular and equant shapes.

Higgins (2006) states that there is a possible relationship between the shape of a crystal and its size. To evaluate this theory, we compared the lengths of studied plagioclase grains in 2D with those of the 3D shapes (Table 3). Contrary to Hastie et al. (2013), the average length of prolate plagioclase crystals in the studied rocks is less than the amount of those in tabular crystals.

The CSD curves for plagioclase from Qisir Dagh are presented in Fig. 11. All of the CSD curves, except the sample

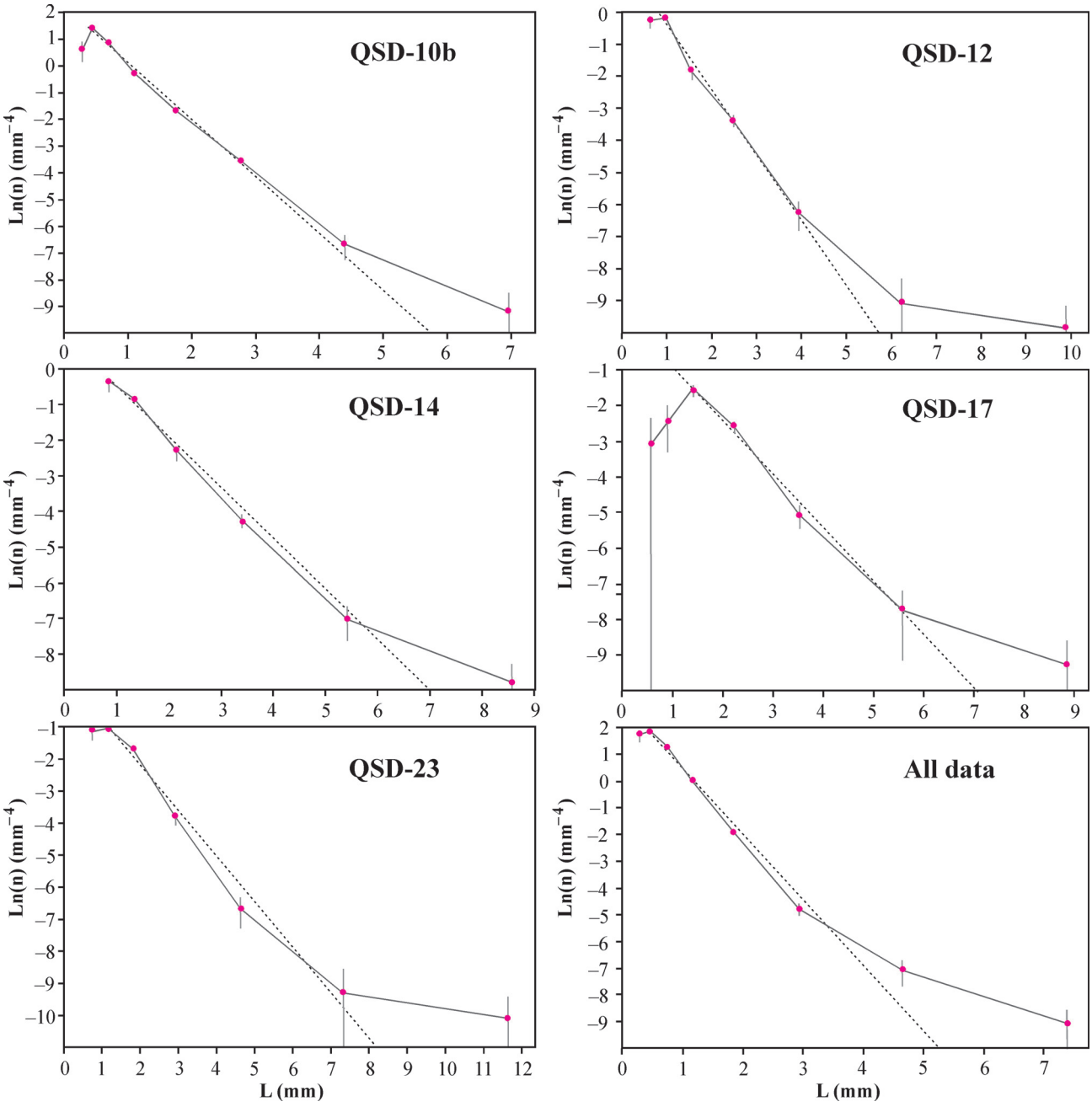

Fig. 11. CSD diagrams of the studied plagioclase crystals from Qisir Dagh. Note the non-linear trend of the diagrams. Dotted lines are the regression lines calculated based on the frequency of all crystal sizes. Horizontal axis unit is millimeter.

Table 4: Calculated residence time for micromonzogabbros of Qisir Dagh based on quantitative textural investigation.

Sample	Residence time (years)	Regression line slope	Regression intercept
QSD-10b	685	–2.16	2.20
QSD-12	621	–1.96	1.48
QSD-14	457	–1.44	0.91
QSD-17	463	–1.46	0.51
QSD-23	460	–1.45	0.71

QSD-10b, are concaved up and do not follow a classic straight line trend. The proportion of larger crystals in the studied rocks is low and their sizes are so variable compared to smaller crystals, which may contribute to the relatively big error of the big segment of CSD curves. The selected regression lines are the ones responsible for the most frequent crystal size intervals (in this case small crystals) that are depicted in CSD curves as the long and straight line in the middle of the curve. These regression lines are drawn based on all the size intervals and since the relatively small crystals are more frequent, these lines mostly follow the segments of CSD curves which are related to these crystals. Taking a simple assumption of plagioclase steady-state magma chamber model and continuous growth rate of 10^{-10} mm/s for gabbroic rocks of dyke structures (Garrido et al. 2001; Cheng & Zeng 2013), the crystal residence times of plagioclase from Qisir Dagh are calculated to be less than 1000 years (Table 4).

Discussion

In almost all of the CSD studies, the interpretations dealing with the cooling conditions of magma have been done on CSD curves. Straight CSD curves form in a simple magma cooling process while non-straight CSD curves indicate occurrence of physico-chemical variations (caused by magma mixing, crystal differentiation, etc.) through magma solidification (e.g. Cashman & Marsh 1988; Higgins 1996, 2000). Comparison of CSD curves of the mircomonzogabbros from Qisir Dagh (Fig. 11) with the standard CSD models of Vinet & Higgins (2010) (Fig. 12) suggests the similarity of CSD curves of this study to the curve presented in Fig. 12e. As mentioned before, CSD curves of the studied samples show notable slope changes and are concave up in shape. Concave up CSD curves are considered to be evidence of hybrid crystal size populations, formed due to magma mixing, crystal differentiation and crystal coarsening (alone or in conjunction) inside magma chamber and/or during magma ascent (Salisbury et al. 2008; Yu et al. 2012; Van der Zwan et al. 2013; Ngonge et al. 2013). Since microscopic studies show no evidence of textural coarsening in the studied rocks, it is likely that magma mixing and/or crystal differentiation played important roles in the formation of plagioclase crystals in Qisir Dagh.

It has been shown by Kouchi et al. (1986) and Higgins (2006) that 3D shapes of crystals have a close relationship with the conditions of magma crystallization. These authors mention that crystallization of magma in a dynamic system and with a high variation in chemical potential produces long and thin crystals. Unequant shape of the studied plagioclase crystals in our study suggests a similar physico-chemical condition.

In addition to quantitative petrographic data, the chemistry of the plagioclase crystals is in accordance with a non-simple magma crystallization trend. Occurrence of exsolution textures in plagioclase as well as their microscopic and chemical attributes point to the influence of chemical and physical processes on the formation of the micromonzogabbros. Temperature, pressure and the amount of K are the most important factors responsible for the development of exsolution textures (particularly antiperthite) in plagioclase. With an increase in temperature and change in the position of O atoms, large K^+ ions can easily replace the Na^+ ions and on cooling form exsolution textures. Alongside the effect of temperature, potassic metasomatism is considered important in forming an exsolution texture (Sen 1959; Bown & Gay 1971; Parsons & Brown 1983). Chemical data of the studied plagioclase suggest the effects of such activities (temperature increasing and potassic metasomatism) through crystallization of the rocks that are also noticeable in CSD curves.

Based on CSD calculations, and using the growth rate $G = 10^{-10}$ mm/s, model residence times of the studied rocks are less than 1000 (457 to 685) years (Table 4). The observed variations in the residence times could be developed in a thermally heterogeneous magma chamber. Short residence times of this range compared to those of coarse grained igneous rocks are believed to be indicative of a low-depth and subvolcanic magmatic system (Cashman 1993) that has formed the microcrystalline rocks of Qisir Dagh. Low residence times justify the microcrystalline texture of the studied rocks and are indicative of formation of the mi-

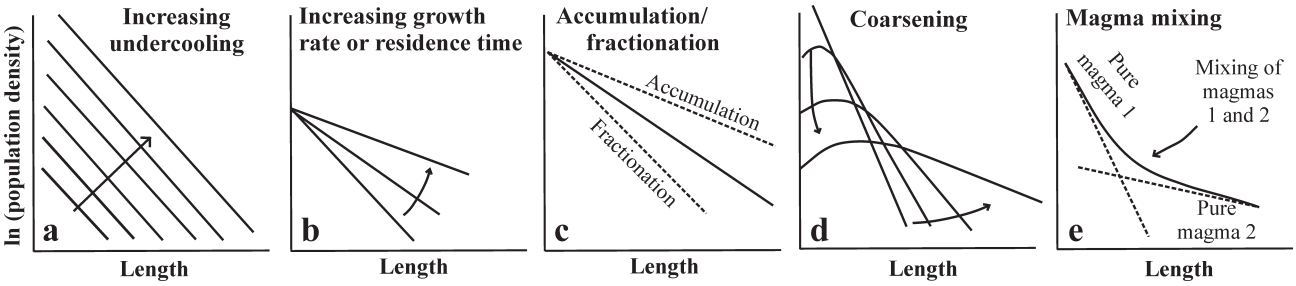

Fig. 12. Schematic examples of processes that can influence the shape of the CSD (after Higgins 2006, modified by Vinet & Higgins 2010). **a** — increase in undercooling (or saturation), **b** — increase in residence time or growth rate, **c** — accumulation and fractionation of crystals, **d** — coarsening, **e** — magma mixing (or mixing of two crystal populations).

cromonzogabbros from Qisir Dagh in a subvolcanic magmatic system (Vernon 2004; Gill 2010).

Conclusions

Results of CSD and mineral chemistry data of micromonzogabbros from Qisir Dagh suggest that:

• Based on measurements of 2266 crystals, the average length size of plagioclase is 538 micrometers which points to the microcrystalline texture of the host rock and its formation in a subvolcanic magmatic system;

• Plagioclase crystals show unequal shapes in intersection dimensions. The size variation of crystal lengths is also more common than the widths which indicates the crystals are unequant;

• The majority of the plagioclase crystals are either prolate or tabular in 3D shape. The average length of prolate plagioclase crystals is less than that in tabular crystals;

• Non-straight and concave up shapes of CSD curves indicate the presence of at least two crystal populations formed as the result of magma mixing and/or crystal differentiation. The process of magma mixing is also supported by the mineral chemistry of plagioclase and the formation of exsolution textures in plagioclase grains;

• Calculated model residence times for plagioclase crystals in Qisir Daghi are less than 457–685 years, using $G = 10^{-10}$ mm/s, indicating rapid cooling in a subvolcanic magmatic system with thermal heterogeneity.

Acknowledgments: The authors would like to thank D.J. Morgan and D.A. Jerram for providing CSDSlice spreadsheet and also H. Altafi, S. Nezamdoost and B. Arefi for their assistance with the field work. Dr. I. Petrík is thanked for editorial handing of the paper and for providing us with valuable scientific comments. Reviews and comments by Prof. H. Yu and an anonymous reviewer are very much appreciated.

References

Ahmadzadeh Gh., Jahangiri A., Lentz D. & Mojtahedi M. 2010: Petrogenesis of Plio–Quaternary post-collisional ultrapotassic volcanism in NW of Marand, NW Iran. *J. Asian Earth Sci.* 39, 1–2, 37–50.

Alberti A.A., Comin-Chiaramonti P., Di Battistini G., Sinigoi S. & Zerbi M. 1975: On the magmatism of the Savalan volcano (north–west Iran). *Rend. Soc. Ital. Mineral. Petrol.* 31, 2, 337–350.

Alberti A.A., Comin-Chiaramonti P., Sinigoi S., Nicoletti M. & Petrucciani C. 1980: Neogene and Quaternary volcanism in Eastern Azerbaijan (Iran): some K–Ar age determinations and geodynamic implications. *Int. J. Earth Sci.* 69, 1, 216–225.

Alberti A.A., Comin-Chiaramonti P., Di Battistini G., Nicoletti M., Petrucciani C. & Sinigoi S. 1976: Geochronology of the Eastern Azerbaijan volcanic plateau (north–west Iran). *Rend. Soc. Ital. Mineral. Petrol.* 32, 2, 579–589.

Allen M.B., Mark D.F., Kheirkhah M., Barfod D., Hashem Emami M. & Saville C. 2011: $^{40}Ar/^{39}Ar$ dating of Quaternary lavas in northwest Iran: constraints on the landscape evolution and incision rates of the Turkish–Iranian plateau. *Geophys. J. Int.* 185, 3, 1175–1188.

Amini B. 1987: Geological Map of Meshginshahr, Scale 1:100,000. *Geol. Surv. Iran Publ.,* Tehran.

Armienti P., Innoncenti F., Pareschi M.T., Pompilio M. & Roscchi S. 1991: Crystal population density in not stationary volcanic systems: Estimate of olivine growth rate in basalts of Lanzarote (Canary Islands). *Miner. Petrology* 44, 3–4, 181–196.

Armstrong J.T. 1988: Quantitative analysis of silicate and oxide minerals: comparison of Monte Carlo, ZAF, and U(qz) procedures. In: Newbury D.E. (Ed.): Microbeam analysis. *Proceedings of the 23rd Annual Conference of the Microbeam Analysis Society*. *San Francisco Press*, San Francisco, 239–246.

Azizi H. & Moinevaziri H. 2009: Review of the tectonic setting of Cretaceous to Quaternary volcanism in northwestern Iran. *J. Geodyn.* 47, 4, 167–179.

Berberian M. & King G.C.P. 1981: Towards a paleogeography and tectonic evolution of Iran. *Canad. J. Earth Sci.* 18, 2, 210–265.

Bown M.G. & Gay P. 1971: Lunar antiperthites. *Earth Planet. Sci. Lett.* 11, 1–5, 23–27.

Cashman K.V. 1993: Relationship between plagioclase crystallization and cooling rate in basaltic melts. *Contr. Mineral. Petrology* 113, 1, 126–142.

Cashman K.V. & Marsh B.D. 1988: Crystal size distribution (CSD) in rocks and the kinetics and dynamics of crystallization. II. Makaopuhi lava lake. *Contr. Mineral. Petrology* 99, 3, 292–305.

Cheng L. & Zeng L. 2013: Nature of subvolcanic magma chambers in Emeishan province, China: evidence from quantitative textural analysis of plagioclase megacrysts in the giant plagioclase basalts. *IAVCEI 2013 Scientific Assembly*, A79.

Cox K.G., Bell J.D. & Pankhurst R.J. 1979: The interpretation of igneous rocks. *George Allen and Unwin*, London, 1–464.

Dabiri R., Hashem Emami M., Mollaei H., Chen B., Vosogi Abedini M., Rashidnejad Omran N. & Ghaffari M. 2011: Quaternary post-collision alkaline volcanism NW of Ahar (NW Iran): geochemical constraints of fractional crystallization process. *Geol. Carpathica* 62, 6, 547–562.

Deer W.A., Zussman J. & Howie R.A. 1992: An introduction to the rock-forming minerals. 2nd ed. *Prentice Hall,* China, 1–712.

Diaz Azpiroz M. & Fernandez C. 2003: Characterization of tectonometamorphic events using crystal size distribution (CSD) diagrams. A case study from the Acebuches metabasites (SW Spain). *J. Struct. Geol.* 25, 935–947.

Didon J. & Gemain Y.M. 1976: Le Sabalan, volcan plio–quaternaire de l'Azerbaidjan oriental (Iran): étude géologique et pétrographique de l'édifice et de son environnement regional. *Unpubl. PhD Thesis, Université Scientifique et Médicale de Grenoble*, France, 1–166.

Dilek Y., Imamverdiyev N. & Altunkaynak Ş. 2010: Geochemistry and tectonics of Cenozoic volcanism in the Lesser Caucasus (Azerbaijan) and the peri-Arabian region: collision-induced mantle dynamics and its magmatic fingerprint. *Int. Geol. Rev.* 52, 4–6, 536–578.

Dostal J. & Zerbi M. 1978: Geochemistry of the Savalan volcano (northwestern Iran). *Chem. Geol.* 22, 31–42.

Gagnevin D., Waight T.E., Daly J.S., Poli G. & Conticelli S. 2007: Insights into magmatic evolution and recharge history in Capraia Volcano (Italy) from chemical and isotopic zoning in plagioclase phenocrysts. *J. Volcanol. Geotherm. Res.* 168, 1–4, 28–54.

Galamghash J., Mousavi Z., Hassanzadeh J. & Schmitt A.K. 2013: Sabalan Volcano, Northwest Iran: Geochemistry and U–Pb zircon geochronology. *Geol. Soc. Amer. Meeting*, A363–9.

Garrido C.J., Kelemen P.B. & Hirth G. 2001: Variation of cooling rate with depth in lower crust formed at an ocean spreading ridge: Plagioclase crystal size distributions in gabbros from the Oman ophiolite. *Geochem. Geophys. Geosystems,* 2. Doi 10.1029/2000GC000136

Gill R. 2011: Igneous rocks and processes, a practical guide. *Wiley-Blackwell*, Malaysia, 1–472.

Hastie W.W., Watkeys M.K. & Aubourg C. 2013: Characterisation of grain-size, shape and orientation of plagioclase in the Rooi Rand dyke swarm, South Africa. *Tectonophysics* 583, 145–157.

Higgins M.D. 1994: Numerical modeling of crystal shapes in thin sections: Estimation of crystal habit true size. *Amer. Mineralogist* 79, 113–119.

Higgins M.D. 1996: Crystal size distributions and other quantitative textural measurements in lavas and tuff from Egmont volcano (Mt. Taranaki), New Zealand. *Bull. Volcanol.* 58, 2–3, 194–204.

Higgins M.D. 2000: Measurement of crystal size distributions. *Amer. Mineralogist* 85, 1105–1116.

Higgins M.D. 2002: A crystal size-distribution study of the Kiglapait layered mac intrusion, Labrador, Canada: evidence for textural coarsening. *Contr. Mineral. Petrology* 144, 3, 314–330.

Higgins M.D. 2006: Verification of ideal semi-logarithmic, lognormal or fractal crystal size distributions from 2D datasets. *J. Volcanol. Geotherm. Res.* 154, 1–2, 8–16.

Innocenti F., Mazzuoli R., Pasquare G., Radicati Di Brozolo F. & Villari L. 1982: Tertiary and quaternary volcanism of the Erzurumkars area (Eastern Turkey): Geochronological data and geodynamic evolution. *J. Volcanol. Geotherm. Res.* 13, 3–4, 223–240.

Innocenti S., Ann del Marmol M., Voight B., Andreastuti S. & Furman T. 2013: Textural and mineral chemistry constraints on evolution of Merapi volcano, Indonesia. *J. Volcanol. Geotherm. Res*. 261, 20–73.

Jahangiri A. 2007: Post-collisional Miocene adakitic volcanism in NW Iran: Geochemical and geodynamic implications. *J. Asian Earth Sci.* 30, 3–4, 433–447.

Jamali H., Yaghubpur A., Mehrabi B., Dilek Y., Daliran F. & Meshkani A. 2012: Petrogenesis and tectono-magmatic setting of Meso–Cenozoic magmatism in Azerbaijan province, Northwestern Iran. In: Al-Juboury A. (Ed.): Petrology — new perspectives and applications. *Intech*, 39–56. ISBN: 978–953–307–800–7

Jerram D.A., Mock A., Davis G.R., Field M. & Brown R.J. 2009: 3D crystal size distributions: A case study on quantifying olivine populations in kimberlites. *Lithos* 112, S1, 223–235.

Kheirkhah M. & Mirnejad H. 2014: Volcanism from an active continental collision zone: a case study on most recent lavas within Turkish–Iranian plateau. *J. Tethys* 2, 2, 81–92.

Kouchi A., Tsuchiyama A. & Sunagawa I. 1986: Effect of stirring on crystallization kinetics of basalt: texture and element partitioning. *Contr. Mineral. Petrology* 93, 4, 429–438.

Lambert R.S.J., Holland J.G. & Owen P.F. 1974: Chemical petrology of a suit of calc-alkaline lavas from Mount Ararat, Turkey. *J. Geology* 82, 4, 419–438.

Marsh B.D. 1988: Crystal size distribution (CSD) in rocks and the kinetics and dynamics of crystallization. I. Theory. *Contr. Mineral. Petrology* 99, 3, 277–291.

McQuarrie N., Stock J.M., Verdel C. & Wernicke B.P. 2003: Cenozoic evolution of Neotethys and implications for the causes of plate motions. *Geophys. Res. Lett.* 30, 20. Doi 10.1029/2003GL017992

Morgan D.J. & Jerram D.A. 2006: On estimating crystal shape for crystal size distribution analysis. *J. Volcanol. Geotherm. Res.* 154, 1–2, 1–7.

Ngonge E.D., Archanjo C.J. & Hollanda M.H.B.M. 2013: Plagioclase crystal size distribution in some mesozoic tholeiitic dykes in Cabo Frio-Buzios, Rio de Janeiro, Brazil. *J. Volcanol. Geotherm. Res.* 255, 26–42.

Parsons I. & Brown W.L. 1983: A TEM and microprobe study of a two-perthite alkali gabbro: implications for the ternary feldspar system. *Contr. Mineral. Petrology* 82, 1, 1–12.

Pazirandeh M. 1973: Distribution of volcanic rocks in Iran and a preliminary discussion of their relationship to tectonics. *Bull. Volcanol.* 37, 4, 573–585.

Pourkhorsandi H. 2014: Geochemistry of subvolcanic rocks from Qisir Dagh, South–East of Savalan volcano, (North–West) Iran. *Unpubl. M.Sc. Thesis, University of Tehran,* Iran, 1–145 (in Farsi).

Randolph A.D. & Larson M.A. 1971: Theory of particulate processes: Analysis and techniques of continuous crystallization. *Academic Press*, New York, 1–268.

Ruprecht P. & Wörner G. 2014: Variable regimes in magma systems documented in plagioclase zoning patterns: El Misti stratovolcano and Andahua monogenetic cones. *J. Volcanol. Geotherm. Res.* 165, 3–4, 142–162.

Ruttner A. & Stöcklin J. 1967: Geological Map of Iran, Scale 1 : 100,000. *Geol. Surv. Iran Publ.,* Tehran.

Sahagian D.L. & Proussevitch A.A. 1998: 3D particle size distributions from 2D observations: stereology for natural applications. *J. Volcanol. Geotherm. Res.* 84, 3–4, 173–196.

Salisbury M.J., Bohrson W.A., Clynne M.A., Ramos F.C. & Hoskin P. 2008: Multiple plagioclase crystal populations identified by crystal size distribution and in situ chemical data: implications for timescales of magma chamber processes associated with the 1915 eruption of Lassen Peak, CA. *J. Petrology* 49, 10, 1755–1780.

Seaman S.J. 2000: Crystal clusters, feldspar glomerocrysts, and magma envelopes in the Atascosa Lookout lava flow, Southern Arizona, USA: recorders of magmatic events. *J. Petrology* 41, 5, 693–716.

Sen S.K. 1959: Potassium content of natural plagioclases and the origin of antiperthites. *J. Geology* 67, 5, 479–495.

Stöcklin J. 1968: Structural history and tectonics of Iran, a review. *Amer. Assoc. Petrol. Geol. Bull.* 52, 7, 1229–1258.

Takin M. 1972: Iranian geology and continental drift in the Middle East. *Nature* 235, 5334, 147–150.

Trifonov V.G., Ivanova T.P. & Bachmanov D.M. 2012: Evolution of the central Alpine–Himalayan belt in the Late Cenozoic. *Russ. Geol. Geophys.* 53, 3, 221–233.

Underwood E.E. 1973: Quantitative stereology for microstructural analysis. In: McCall J.L. & Mueller W.M. (Eds.): Microstructural analysis, tools and techniques. *Plenum Press*, New York, 35–66.

Ustunisik G., Kilinc A. & Nielsen R.L. 2014: New insights into the processes controlling compositional zoning in plagioclase. *Lithos* 200–201, 80–93.

Van der Zwan F.M., Chadwick J.P. & Troll V.R. 2013: Textural history of recent basaltic-andesites and plutonic inclusions from Merapi volcano. *Contr. Mineral. Petrology* 166, 1, 43–63.

Vernon R.H. 2004: A practical guide to rock microstructures. *Cambridge University Press,* New York, 1–655.

Vinet N. & Higgins M.D. 2010: Magma solidification processes beneath Kilauea volcano, Hawaii: a quantitative textural and geochemical study of the 1969–1974 Mauna Ulu lavas. *J. Petrology* 51, 6, 1297–1332.

Winkeler H.G.F. 1949: Crystallization of basaltic magma as recorded by variation of crystal-size in dikes. *Mineral. Mag.* 28, 557–574.

Yilmaz Y., Moorbath F. & Mitchell J.G. 1990: Genesis of collision volcanism in Eastern Anatolia, Turkey. *J. Volcanol. Geotherm. Res.* 44, 1–2, 189–229.

Yu H., Xu J., Lin C., Shi L. & Chen X. 2012: Magmatic processes inferred from chemical composition, texture and crystal size distribution of the Heikongshan lavas in the Tengchong volcanic eld, SW China. *J. Asian Earth Sci.* 58, 1–15.

Zingg Th. 1935: Beitrag zur Schotteranalyse. *Unpubl. PhD Thesis*, *Universität Zürich,* Switzerland, 1–140.